

# SPI/INTEGRAL OBSERVATION OF 1809 KEV GAMMA-RAY LINE EMISSION FROM THE CYGNUS X REGION

J. Knödlse<sup>1</sup>, M. Valsesia<sup>3,4</sup>, M. Allain<sup>1</sup>, S. Boggs<sup>5</sup>, R. Diehl<sup>2</sup>, P. Jean<sup>1</sup>, K. Kretschmer<sup>2</sup>, J.-P. Roques<sup>1</sup>, V. Schönfelder<sup>2</sup>, G. Vedrenne<sup>1</sup>, P. von Ballmoos<sup>1</sup>, G. Weidenspointner<sup>1</sup>, and C. Winkler<sup>6</sup>

<sup>1</sup>Centre d'Étude Spatiale des Rayonnements, B.P. 4346, 31028 Toulouse Cedex 4, France (knodlseder@cesr.fr)

<sup>2</sup>Max-Planck-Institut für extraterrestrische Physik, Postfach 1312, 85741 Garching, Germany

<sup>3</sup>IASF - CNR, via Bassini 15, 20133 Milan, Italy

<sup>4</sup>Università di Pavia, Dipartimento di Fisica, via Bassi 6, 27100 Pavia, Italy

<sup>5</sup>SSL, University of California Berkeley, CA 94720, USA

<sup>6</sup>ESA-ESTEC, Keplerlaan 1, 2201 AZ Noordwijk, The Netherlands

## ABSTRACT

We present first results on the observation of 1809 keV gamma-ray line emission from the Cygnus X region with the SPI imaging spectrometer. Our analysis is based on data from the performance verification phase of the INTEGRAL instruments and comprises 1.3 Ms of exposure time. We observe a 1809 keV line flux of  $(7.3 \pm 0.9) \times 10^{-5}$  ph cm<sup>-2</sup>s<sup>-1</sup> from a region delimited by galactic longitudes 73°-93° and  $|b| \leq 7^\circ$  at a significance level of  $8\sigma$ . The 1809 keV line appears moderately broadened, with an intrinsic FWHM of  $3.3 \pm 1.3$  keV. Although this broadening is only marginal (at the  $2\sigma$  level our data are compatible with an unbroadened line), it could reflect the <sup>26</sup>Al ejecta kinematics.

Key words: gamma rays; observations; stars: O-type, Wolf-Rayet; supernovae; nucleosynthesis.

is produced in this region during hydrostatic nucleosynthesis in O-type and Wolf-Rayet stars; explosive nucleosynthesis in core collapse supernovae seems to play only a minor role. Yet, the measured 1809 keV intensity is by at least a factor of 2 larger than expected from current nucleosynthesis models (Knödlse<sup>1</sup> et al., 2002). This may hint at an enhanced efficiency of hydrostatic <sup>26</sup>Al nucleosynthesis, such as expected for rotationally induced mixing in fast rotating O-type stars (Vuissoz et al., 2004). Any nucleosynthesis process that is at work in Cygnus should in principle also hold for the entire Galaxy. Hence Cygnus X may turn out to become the Rosetta stone for understanding <sup>26</sup>Al nucleosynthesis galaxywide. It is therefore particularly important to accurately measure the 1809 keV gamma-ray line emission from this region, to precisely determine its intensity, to identify emission counterparts, and to study the line profile that holds information about <sup>26</sup>Al ejecta dynamics.

## 1. INTRODUCTION

The Cygnus X region is one of the most active nearby star forming regions in our Galaxy (Knödlse<sup>1</sup>, 2003). It houses an exceptionally large number of O-type stars that enrich the interstellar medium with fresh nucleosynthesis products, either through their strong stellar winds, or eventually through their final supernova explosions. The radioactive isotope <sup>26</sup>Al is a key tracer of this process, and the study of its 1809 keV decay radiation is a powerful probe for nucleosynthesis in this region.

COMPTEL measurements have revealed the presence of <sup>26</sup>Al in Cygnus X (Del Rio et al., 1996; Plüschke, 2001). A deep study of the stellar populations in the Cygnus field suggests that most <sup>26</sup>Al

## 2. ANALYSED DATA

The data that we analysed in this work were taken during the INTEGRAL performance verification phase. They span the INTEGRAL orbits 14-25 (excluding orbit 24), covering 1.3 Ms exposure time. We analyse single-detector and double-detector data (SE and ME2). Energy calibration has been performed orbit-wise, resulting in a relative (orbit-to-orbit) calibration precision of  $\sim 0.01$  keV and an absolute accuracy of  $\sim 0.05$  keV (Lonjou et al., these proceedings).

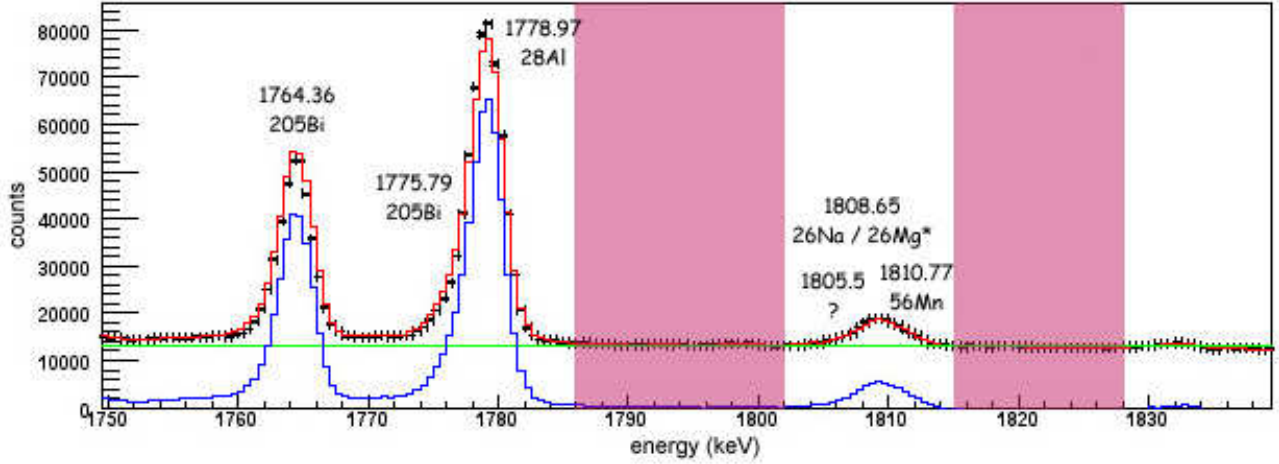


Figure 1. SPI single-detector spectrum in the area around 1809 keV together with the background model. (black/red histogram: line component; light/green line: continuum component; grey/red histogram: summed model). The shaded areas indicate the energy bands that have been used for modelling the continuum emission underlying the line. Instrumental background lines have been labelled by their source isotopes.

### 3. BACKGROUND MODELLING

The instrumental background of the SPI telescope at 1809 keV is composed of a broad line complex on top of a flat continuum distribution (cf. Fig. 1). The 1809 keV complex is a blend of at least 3 individual lines: a yet unidentified component at about  $1805.5 \pm 0.5$  keV, a line at the  $^{26}\text{Al}$  rest energy of 1808.65 keV attributed to  $^{26}\text{Na}(\beta^-)^{26}\text{Mg}^*$  decay and to excitation of  $^{26}\text{Mg}$  nuclei, and a line at 1810.77 keV attributed to  $^{56}\text{Mn}(\beta^-)^{56}\text{Fe}$  decay (Weidenspointner et al., 2003). The relative contributions of each of the lines to the complex amount to roughly 10%, 60% and 30%, respectively, and appear stable with time.

We model the energy and time dependence of the instrumental background using a two component model that allows for different time variabilities of line and continuum background. The line component is predicted from empty field observations that are assumed to be free of celestial 1809 keV emission. For this purpose, a total empty field exposure of 4.1 Ms has been collected by gathering all data for which SPI pointed at galactic latitudes  $|b| > 20^\circ$  (covering INTEGRAL orbits 14-106). The spectra for this observation are summed for all detectors, and the line component is extracted by subtracting a constant offset whose level has been estimated from the adjacent energy bands 1786-1802 keV and 1815-1828 keV. The time dependent counting rate of the line component has been modelled by adjusting a multi-component background variation template to the counting rate history of the empty field data. The components of the template reflect our current knowledge about the physical processes that give rise to the 1809 keV line complex (see also Knödseder et al., these proceedings).

The continuum component was assumed to be constant in energy (note that we also used a constant to extract the line component from the empty field

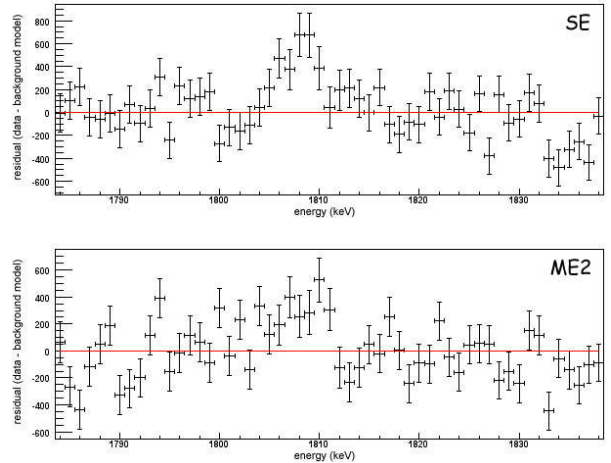


Figure 2. Residual SE and ME2 SPI energy spectra after subtraction of the background model. For the SE spectrum a degradation correction has been applied (section 4).

data, hence the line and continuum components are complementary and the sum of both should add without bias). Its time dependent counting rate has been estimated by adjusting the germanium saturated event rate as activity tracer to the counting rate in adjacent energy bands (the same intervals have been used as for the extraction of the line component from the empty field data). The adjustment has been performed using an adaptive running average that requires at least 10000 counts in the adjacent bands. In this way, short term variabilities are explained by the activity tracer while long term variations come from the data themselves.

Figure 2 shows the background subtracted spectra for single-detector and double-detector events. Clearly, a residual signal remains at 1809 keV in the spectra of both event types.

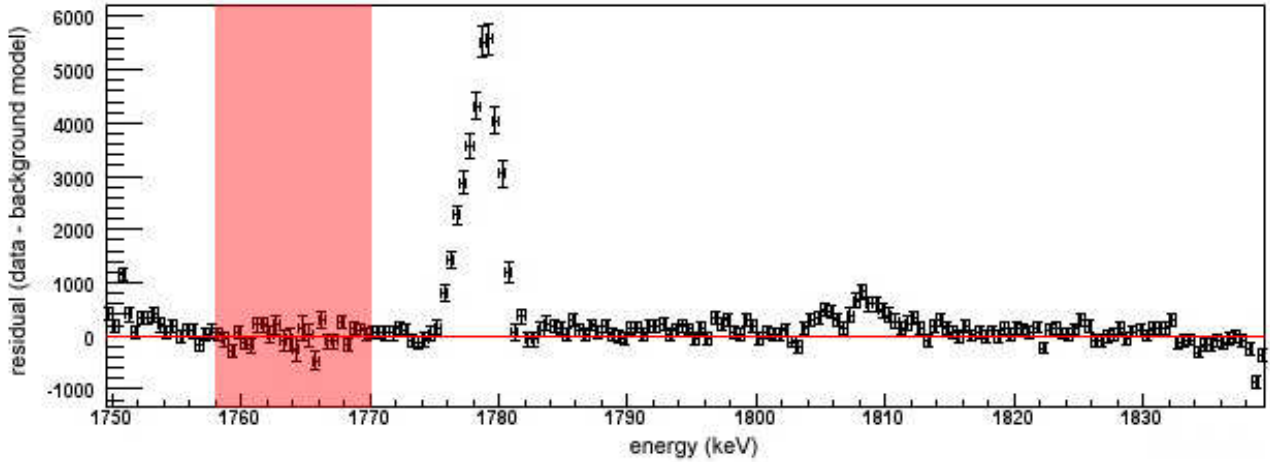


Figure 3. SE residual spectrum after degradation correction, based on a  $\chi^2$  minimisation of the residuals in the energy interval 1758-1770 keV (this energy band is indicated by a shaded area).

#### 4. DEGRADATION CORRECTION

The exposure of the SPI camera to high-energy particle radiation in space leads to a degradation of the energy resolution with time due to creation of trapping sites in the germanium crystals (Leleux et al., 2003). These defects are regularly removed using an annealing procedure (Roques et al., 2003). Since the empty field observations used for modelling the shape of the instrumental 1809 keV line complex were taken at different epochs than the source data, and hence at different detector degradations, the shape of the instrumental line differs slightly between the source data and the background model. A close look to Fig. 1 reveals indeed that the background model shows broader lines than the source data (detector degradation leads to an extension of the left wing of a line due to incomplete charge collection).

To match the spectral shape of source data and background model, we therefore reassign energies  $E \rightarrow E'$  for each event using a random number generator that follows the probability density function

$$p(E'|E) = \frac{1}{\Delta E} e^{-(E-E')/\Delta E} \quad (1)$$

where  $E' \leq E$  (i.e. incomplete charge collection) and  $\Delta E$  characterises the detector degradation. Since Eq. 1 effectively decreases the energy of each event (by  $\Delta E$  on average) the background model has to be shifted to lower energies in order to match the data. Also, a recalibration of the data is required after this correction, that we perform using the 1764.36 keV background line of  $^{205}\text{Bi}$ .

The degradation constant  $\Delta E$  and the background shift were determined for each detector by minimising the residuals in the 1764.36 keV background line. This has been done using a  $\chi^2$  minimisation applied to the energy interval 1758-1770 keV. The resulting average degradation correction amounted to  $\Delta E \approx 0.5$  keV, the average shift of the background

model was  $-0.3$  keV. The corrected SE residual spectrum is shown in Fig. 3. Note that the background model components were scaled by the fitting algorithm for  $\chi^2$  minimisation and visual display since the normalisation of the 1764.36 keV line differs from those of the other background lines due to a different time history (without scaling the spectrum could never become flat). For this reason a strong residual remains in Fig. 3 at 1779 keV and also the residual 1809 keV line signal is exaggerated. For data analysis, however, no scaling has been applied to the background model.

Remaining residuals of the 1764.36 keV line are of the order of 1% of the instrumental background line. The expected celestial 1809 keV signal amounts to  $\sim 12\%$  of the counts in the 1809 keV complex. Assuming that the background subtraction leaves also 1% residuals at 1809 keV, we estimate residuals from instrumental background that amount to  $\sim 10\%$  of the celestial 1809 keV signal.

#### 5. SPECTRAL ANALYSIS

Straight background spectra subtraction does not make use of the coded-mask and field-of-view properties of SPI; on the other hand, image deconvolution is feasible only for strong signals. As we expect a weak signal, we derive spectra by fitting the amplitude of a given skymap of (expected) intensity distribution, per 1 keV wide energy bin. As skymap we used the Dirbe 240  $\mu\text{m}$  intensity distribution, since this map has been shown to provide a reasonable tracer of galactic 1809 keV emission (Knödseder et al., 1999).

Figure 4 shows the resulting SE and ME2 spectra. Fitting Gaussian shaped lines on top of a constant provides flux, line position and line width estimates that are summarised in Table 1. The results for SE and ME2 have been combined by weighting with the statistical uncertainties. The line position and width

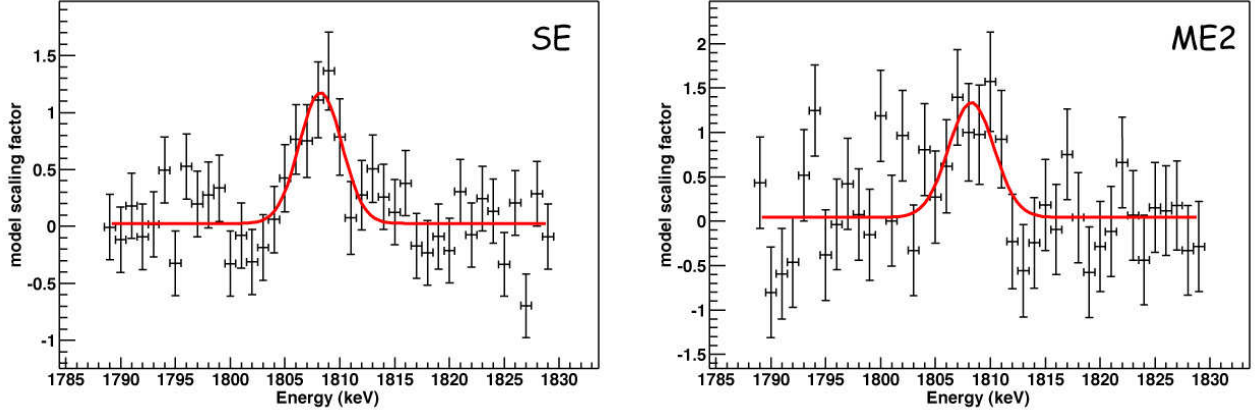


Figure 4. SPI SE and ME2 spectra of the Cygnus X region assuming an  $^{26}\text{Al}$  line intensity distribution that follows the Dirbe  $240\ \mu\text{m}$  infrared emission as a tracer of the massive star population.

Table 1. Spectral analysis results. The flux is given in units of  $10^{-5}\ \text{ph cm}^{-2}\text{s}^{-1}$  and has been determined by integrating over galactic longitudes  $70^\circ$ - $93^\circ$  and latitudes  $b \leq 7^\circ$ . The energy and intrinsic line width are given in units of keV.

Events	Flux	Energy	FWHM
SE	$6.7 \pm 2.3$	$1808.4 \pm 0.4$	$3.2 \pm 1.7$
ME2	$8.1 \pm 3.1$	$1808.4 \pm 0.7$	$3.4 \pm 2.4$
Sum	$7.2 \pm 1.8$	$1808.4 \pm 0.3$	$3.3 \pm 1.3$

values are given after degradation correction and recalibration. The line width is the intrinsic value after (quadratic) subtraction of the instrumental line widths. The instrumental widths have been determined from the width of the  $1764.36\ \text{keV}$  background line (after degradation correction and recalibration) which is known to be intrinsically narrow. We obtain instrumental FWHMs of  $3.2$  and  $3.5\ \text{keV}$  for SE and ME2, respectively.

## 6. DISCUSSION AND CONCLUSIONS

The measured  $1809\ \text{keV}$  line flux corresponds well to previous COMPTEL measurements. From two years of COMPTEL data, Del Rio et al. (1996) derived a flux of  $(7.0 \pm 1.4) \times 10^{-5}\ \text{ph cm}^{-2}\text{s}^{-1}$  from a sky region covering  $l = [73^\circ, 93^\circ]$  and  $b = [-7^\circ, 7^\circ]$ , corresponding to a detection significance of  $5\sigma$ . Integrating the fitted Dirbe  $240\ \mu\text{m}$  map over the same area results in a SPI value of  $(7.2 \pm 1.8) \times 10^{-5}\ \text{ph cm}^{-2}\text{s}^{-1}$ . Our quoted flux uncertainty also includes the uncertainty in the line width. Neglecting the line width uncertainty by analysing SPI data in single energy bands leads to a flux value of  $(7.3 \pm 0.9) \times 10^{-5}\ \text{ph cm}^{-2}\text{s}^{-1}$ , corresponding to a SPI detection significance of  $8\sigma$ .

From the analysis of 9 years of COMPTEL data, Plüschke (2001) derived a flux of  $(10.3 \pm 2.0) \times 10^{-5}\ \text{ph cm}^{-2}\text{s}^{-1}$  from a slightly larger sky region covering  $l = [70^\circ, 96^\circ]$  and  $b = [-9^\circ, 25^\circ]$ . For the same region we find a value of  $(10.0 \pm 2.6) \times 10^{-5}\ \text{ph cm}^{-2}\text{s}^{-1}$  from the spectral analysis, and  $(10.3 \pm 1.3) \times 10^{-5}$  from the single energy band analysis. Thus, our flux measurements are consistent with earlier COMPTEL results, and although only  $1.3\ \text{Ms}$  of exposure time have been analysed so far, they present the most precise measurements of the  $1809\ \text{keV}$  line intensity from Cygnus X that is available today.

SPI measured for the first time the precise energy of the  $1809\ \text{keV}$  line towards Cygnus, and the resulting value of  $1808.4 \pm 0.3\ \text{keV}$  is compatible with the rest energy of the  $^{26}\text{Al}$  line at  $1808.65\ \text{keV}$ . When interpreted kinematically, the SPI measurement corresponds to a radial velocity of  $-41 \pm 50\ \text{km s}^{-1}$  which is compatible with the radial velocity of  $\sim 0\ \text{km s}^{-1}$  of massive star clusters found in Cygnus X (Knödlseher, 2003).

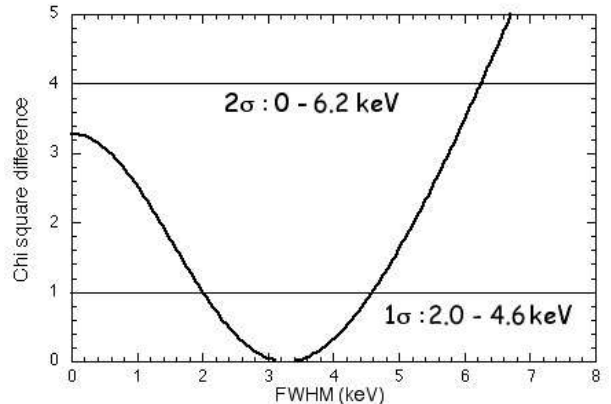


Figure 5.  $\chi^2$  of the combined SE and ME2 spectral fit as function of intrinsic  $1809\ \text{keV}$  line width.

SPI also provides for the first time an estimate of the intrinsic width of the  $1809\ \text{keV}$  line in Cygnus X. Figure 5 shows the  $\chi^2$  of the combined fit of SE and

ME2 spectra as function of the intrinsic line width. No significant (i.e. more than  $3\sigma$ ) line broadening can be claimed from the present data, yet there are hints for a modest broadening. The formal line width of  $3.3 \pm 1.3$  keV corresponds to a Doppler broadening of  $550 \pm 210$  km s<sup>-1</sup> (FWHM). This translates into expansion velocities of 170-380 km s<sup>-1</sup> if a thin expanding shell is assumed, or to 240-550 km s<sup>-1</sup> for a homologously expanding bubble.

These values are relatively high with respect to expansion velocities of a few tens of km s<sup>-1</sup> that would have been expected from wind blown bubble expansion in Cygnus X (Knödlseider, 2003). Galactic rotation can also not explain this broadening since the velocity dispersion in this area of the Galaxy is quite small (also only a few tens of km s<sup>-1</sup>). Yet turbulent motions in hot superbubbles can reach velocities of a few 100 km s<sup>-1</sup> (De Avillez, private communication), and the <sup>26</sup>Al ejecta may eventually follow these motions. However, more observations of Cygnus X are required to confirm this hypothesis, by providing more stringent informations on the <sup>26</sup>Al line profile. More observations of Cygnus X have been executed during the INTEGRAL AO-1 cycle, and further observations are scheduled for AO-2. In the near future it can therefore be expected that SPI will provide a more constraining measure of the <sup>26</sup>Al line width, providing valuable information on the <sup>26</sup>Al ejecta dynamics and the ISM kinematics in the Cygnus X region.

## REFERENCES

- Del Rio, E., et al. 1996, A&A, 315, 237  
 Knödlseider, J. 2003, Proc. IAUS 212, eds. K. van der Hucht, A. Herrero, and E. Cesar, p. 505  
 Knödlseider, et al. 2002, A&A, 390, 945  
 Knödlseider, et al. 1999, A&A, 344, 68  
 Leleux, P., et al. 2003, A&A, 411, L85  
 Plüschke, S. 2001, PhD thesis, TU Munich  
 Roques, J.-P., et al. 2003, A&A, 411, L91  
 Vuissoz, C., et al. 2004, New Astronomy Rev., 48, 7  
 Weidenspointner, G., et al. 2003, A&A, 411, 113